Petrogenesis of Early Cretaceous adakites from the Liaodong Peninsula: insight into the lithospheric thinning of the North China Craton

Chao Wang[1,2], Jinlei Sun[1,3], Yanjie Shen[1,4], Tao Tian[5], Jinyu Li[1,6], Ye Qian[1,4] and Fengyue Sun[1,4]

[1]College of Earth Sciences, Jilin University, No. 2199 Jianshe Street, Changchun 130061, China; [2]Jilin Institute of Geological Survey, Changchun 130061, China; [3]State Key Laboratory of Ore Deposit Geochemistry, Institute of Geochemistry, Chinese Academy of Sciences, Guiyang 550081, China; [4]Key Laboratory of Mineral Resources Evaluation in Northeast Asia, Ministry of Nature Resources of China, No. 2199 Jianshe Street, Changchun 130061, China; [5]The Fifth Geological Exploration Institute of Qinghai Province, No. 42 Chaoyang West Street, Xining 810000, China and [6]State Key Laboratory of Geological Processes and Mineral Resources, China University of Geosciences, Wuhan 430074, China

Abstract

Lithospheric thinning occurred in the North China Craton (NCC) that resulted in extensive Mesozoic magmatism, which has provided the opportunity to explore the mechanism of the destruction of the NCC. In this study, new zircon U–Pb ages, geochemical and Lu–Hf isotopic data are presented for Early Cretaceous adakitic rocks in the Liaodong Peninsula, with the aim of establishing their origin as well as the thinning mechanism of the NCC. The zircon U–Pb data show that crystallization occurred during 127–120 Ma (i.e. Early Cretaceous). These rocks are characterized by high Sr (294–711 ppm) content and Sr/Y ratio (38.5–108), low Yb (0.54–1.24 ppm) and Y (4.9–16.4 ppm) contents, and with no obvious Eu anomalies, implying that they are adakitic rocks. They are enriched in large-ion lithophile elements (e.g. Ba, K, Pb and Sr) and depleted in high-field-strength elements (e.g. Nb, Ta, P and Ti). These adakitic rocks have negative zircon $\epsilon_{Hf}(t)$ contents (−28.9 to −15.0) with two-stage Hf model ages (T_{DM2}) of 3004–2131 Ma. Based on the geochemical features, such as low TiO_2 and MgO contents, and high La/Yb and K_2O/Na_2O ratios, these adakites originated from the partial melting of thickened eclogitic lower crust. They were in an extensional setting associated with the slab rollback of the Palaeo-Pacific Ocean. In combination with previous studies, as a result of the rapid retracting of the Palaeo-Pacific Ocean during 130–120 Ma, the asthenosphere upwelled and modified the thickened lithospheric mantle, which lost its stability, resulting in the lithospheric delamination and thinning of the NCC.

1. Introduction

The North China Craton (NCC) is one of the oldest known cratons in China, and has a unique evolutionary history. Based on the research of mantle xenoliths from the Palaeozoic kimberlites and Cenozoic basalts, the NCC underwent reactivation and dramatic lithospheric thinning (> 100 km) (Griffin *et al.* 1998; Fan *et al.* 2000; Menzies *et al.* 2007; Zhu *et al.* 2011; Wu *et al.* 2019). Although some understanding of lithospheric thinning in the NCC has been obtained by petrology, geochemistry and geophysics, the initial timing and geodynamics mechanism are still controversial (Wu *et al.* 2005a, 2008; Zhai *et al.* 2007). The initial timing of thinning and destruction of the NCC ranges from Late Triassic (Duan *et al.* 2014) to Late Jurassic (Jiang *et al.* 2010) and Early Cretaceous (Wu *et al.* 2008). Regarding the geodynamics mechanism, there exist delamination (Deng *et al.* 1994, 2007; Gao *et al.* 2002, 2004; Xu *et al.* 2006a, b; Windley *et al.* 2010) and thermo-chemical erosion (Menzies *et al.* 1993; Xu *et al.* 2004; Zheng *et al.* 2006) models.

Adakites were first proposed by Defant & Drummond (1990) on the basis of their geochemical features (e.g. high Sr/Y and La/Yb ratios; low Y and Yb contents). Scholars proposed that adakites may have originated from either: partial melting of hot subducted oceanic crust (Defant & Drummond, 1990); partial melting of the thickened lower crust (Muir *et al.* 1995); or assimilation and fractional crystallization (AFC) processes associated with basaltic magma (Castillo *et al.* 1999), the reaction of delaminated lower crust with mantle peridotite (Gao *et al.* 2004) or the mixing of basaltic and felsic magmas (Guo *et al.* 2007). The various origins of adakites play a critical role in understanding the growth and evolution of the crust (Guo *et al.* 2006). Large-scale Mesozoic magmatism is one type of geological evidence of the lithospheric thinning and destruction of the NCC (Wu *et al.* 2005a; Xu *et al.* 2009; Yang *et al.* 2009). It is noteworthy that a large number of adakitic rocks (c. 175–110 Ma) have been identified from the

Mesozoic magmatic activity, distributed along the edge of the NCC (Fig. 1a; Zhang & Wang, 2001; Xiong *et al.* 2011). Because the age and distribution of adakites are consistent with the thinning range of the NCC, the age, source and origin of adakites can provide an important window into the processes and mechanisms of lithospheric thinning and destruction of the NCC.

The Liaodong Peninsula is one of the most important parts of the NCC, which also underwent complex magmatic activity and dramatic lithospheric thinning (Fig. 1b; Zhu *et al.* 2011). Studies shown that a large number of Mesozoic magmatic rocks, such as A-type granite, mafic rocks, calc-alkaline I-type rocks and adakites, are distributed in the Liaodong Peninsula (Wu *et al.* 2008; Liu *et al.* 2011, 2013; Wang *et al.* 2015). These Mesozoic rocks indicate that it is an important place to study the thinning of the NCC. Previous studies on these rocks have obtained some periodic results (Yang *et al.* 2004, 2012; Wu *et al.* 2008; Duan *et al.* 2014). However, the geodynamics setting of Early Cretaceous magmas still remains controversial (Sun *et al.* 2007; Xiao *et al.* 2010; Zhu *et al.* 2011; Zhang, 2013). Recently, we discovered a set of Early Cretaceous magmatic rocks with adakitic features in Liaodong Peninsula (Fig. 2). In this paper, we use major- and trace-element compositions, zircon U–Pb ages and Hf isotopes to restrict their magma sources and origin. Our aim is to reveal the tectonic dynamic setting of the Early Cretaceous magmatic rocks in the Liaodong Peninsula, and provide new evidence for the mechanism of lithospheric thinning and destruction of the NCC.

2. Geological setting and sample descriptions

The NCC is triangular in shape, with the Central Asian Orogenic belt, and the Qinling–Dabie and Sulu high–ultrahigh-pressure metamorphic belts, located to its north, south and east, respectively (Fig. 1a; Zhao *et al.* 2005; Liu *et al.* 2020). The NCC was formed as a result of the collision between eastern and western blocks along the central orogenic belt during the Palaeoproterozoic Era (*c.* 1.85 Ga; Zhao *et al.* 2005; Zhai & Santosh, 2011), after which the NCC remained relatively stable and formed sedimentary basins and thick sedimentary rocks. The NCC then began to activate during the Mesozoic Era, which resulted in the thinning and destruction of the lithosphere, and the formation of a large number of ore deposits, magmatic rocks and extensional structures (Wu *et al.* 2005*a*; Zhu *et al.* 2012; Zhu & Xu, 2019).

Located in the eastern part of the NCC (Fig. 1a), the Liaodong Peninsula can be divided into three tectonic units: the Archean Liaobei block in the north, the Archean Liaonan block in the south and the Palaeoproterozoic Jiao-Liao-Ji orogenic belt (JLJOB) in the middle (Liu *et al.* 1992; Wu *et al.* 2005*b*). The basement rocks mainly consist of Early Archean tonalite, trondhjemite and granodiorite (TTG) suites in the Liaobei block; Late Archean diorite, tonalite and granodiorite in the Liaonan block; and Palaeoproterozoic Liaohe Group in the JLJOB (Lu, 2004; Wu *et al.* 2005*b*). These basement rocks were then covered by Mesoproterozoic–Palaeozoic sedimentary strata (Yang *et al.* 2007*b*). The reactivation of the NCC resulted in the widespread distribution (*c.* 20 000 km^2) of Mesozoic intrusive rocks in the Liaodong Peninsula (Fig. 1b; Yang *et al.* 2007*b*). These Mesozoic magmatic rocks, consisting of syenite, monzogranite, granodiorite and diorite, were mainly deposited during three episodes: (1) Late Triassic (mainly 230–210 Ma); (2) Jurassic (mainly 180–155 Ma); and (3) Early Cretaceous (mainly 131–106 Ma) (Li, 2019). In addition, minor Mesozoic mafic dykes also occur in in the Liaodong Peninsula (Fig. 1b).

The Pulandian area covers an area of about 17 km^2 and is distributed in the western part of the Liaodong Peninsula (Fig. 1b). The Precambrian basement is mainly composed of Neoarchean gneissic complex (e.g. biotite plagioclase gneiss) and Mesoproterozoic quartz diorite (Fig. 2). The intrusive rocks are mainly composed of intermediate-acidic rocks, which include monzodiorite, granodiorite, porphyritic monzogranite and monzogranite. In this study, these intermediate-acidic rocks were collected in the Pulandian area for research (Fig. 2).

The monzodiorite (sample no. Yd2005) is grey-white in colour and contains plagioclase (50–55%), biotite (15–20%), K-feldspar (5–10%), quartz (5–10%) and minor hornblende (*c.* 5%) (Fig. 3a–c). Typical polysynthetic twinning can be seen in plagioclases (Fig. 3c). The granodiorite (sample nos Yd2006 and Yd2010) is medium-grained and comprises plagioclase (45–50%), K-feldspar (20–25%), quartz (15–20%) and minor hornblende and biotite (*c.* 5%) (Fig. 3d–i). Small amounts of fine-grained biotite and hornblende are found in the margins of large-grained plagioclase and quartz. Sample Yd2010 contains minor perthite (Fig. 3i). The porphyritic monzogranite (sample no. Yd2009) has porphyritic texture, consisting of phenocryst (*c.* 15%) and matrix (*c.* 85%) (Fig. 3j–l). The phenocryst mainly consists of quartz, K-feldspar, plagioclase and biotite (Fig. 3l). The matrix is composed of fine-grained plagioclase, quartz and minor biotite.

3. Analytical methods

3.a. Zircon U–Pb dating

Zircons were separated from samples by magnetic and heavy-liquid separation methods at Langfang Hongxin Geological Exploration Technology Service Co. Ltd, Hebei Province, China. Zircons were observed and imaged to reveal their internal structure under cathode-luminescence (CL). Zircon laser ablation inductively coupled plasma mass spectrometry (LA-ICP-MS) U–Pb dating was conducted at the Laboratory of Mineral Resources Evaluation in Northeast Asia, Ministry of Nature Resources of China, Changchun (LMRENA), using a 193 nm ArF laser ablation system and Agilent 7900 ICP-MS. The denudation frequency and spot diameter of laser were 7 Hz and 32 µm, respectively. Standard zircon 91500 was adopted as the external standard for age calibration. These 91500 zircons yield a $^{206}Pb/^{238}U$ age range 1060.9–1069.1 Ma, with weighted mean 1065.0 Ma, which is consistent with the recommended values of 1064 Ma for 91500 zircons within analytical errors. NIST610 was used as an external standard and ^{29}Si as an internal standard to normalize zircon trace-element contents. The isotope ratio was calculated using the LA-ICP-MS DATECAL program (Liu *et al.* 2008). Pb correction methods according to Andersen (2002) were followed. The calculated age and Concordia diagrams were calculated using the Isoplot3 program (Ludwig, 2003).

3.b. Major- and trace-element analysis

Whole-rock major- and trace-element geochemical analyses were undertaken at LMRENA. Altered surfaces were removed from all samples and were ground to 200 mesh. The X-ray fluorescence (XRF) and ICP-MS were used for major- and trace-element testing, respectively. The trace-element analytical samples were prepared by dissolving in mixed acid (HF + HNO$_3$) in Teflon bombs. The national standards GBW07103 and GBW07105 were
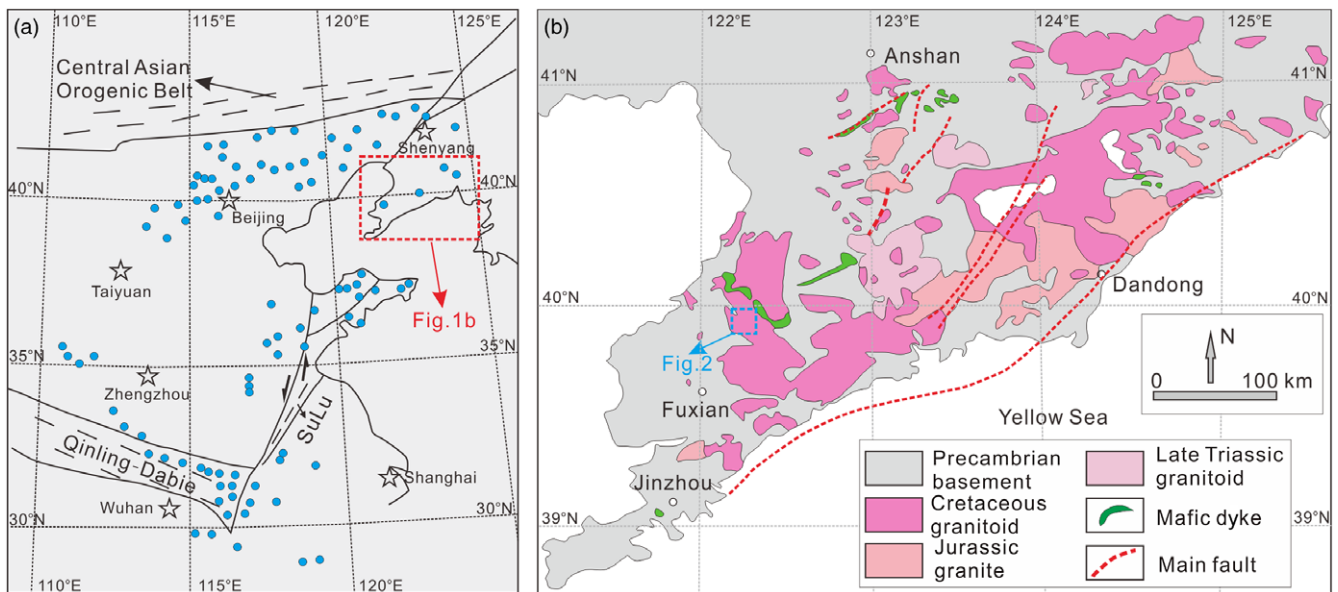
Fig. 1. (Colour online) (a) Distribution of Mesozoic adakites (ages mainly 175–110 Ma) in the eastern NCC (after Zhang & Wang, 2001; Xiong *et al*. 2011); and (b) geological map and distribution of Mesozoic magmatic rocks in the Liaodong Peninsula (modified after Wu *et al*. 2005b; Yang *et al*. 2007a).
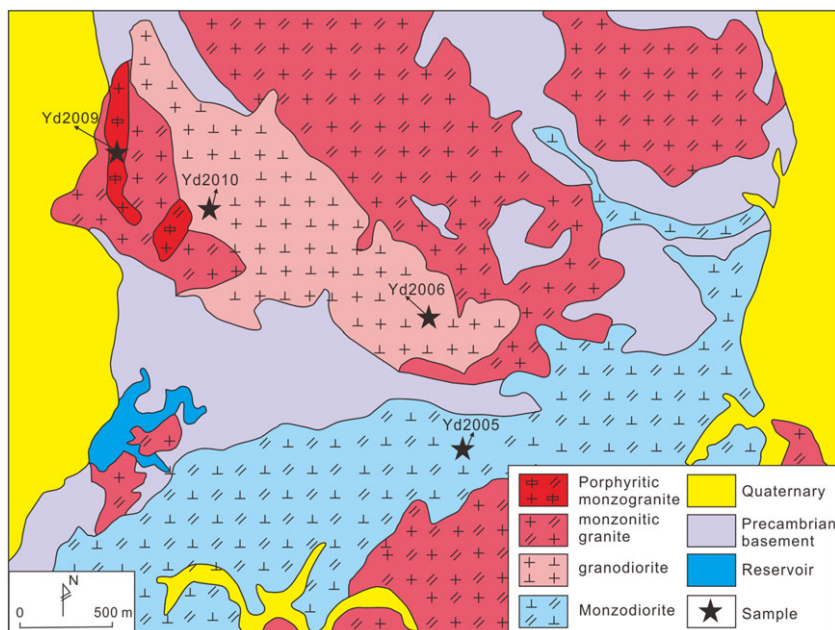

Fig. 2. (Colour online) Geological sketch map of the Pulandian region with sample locations.

adopted for element content correction. The analytical precision of major- and trace-element testing was 1% and 5%, respectively.

3.c. Zircon Hf isotopic analyses

Zircon *in situ* Lu–Hf isotope analyses were conducted using a Neptune-plus multicollector (MC) ICP-MS and NewWave UP213 laser ablation system at Yanduzhongshi Geological Analysis Laboratory, Beijing. The denudation frequency and spot diameter of the laser were 8 Hz and 50 μm, respectively. Standard zircons (e.g. GJ-1, Mud Tank, Penglai and 91500) were treated as precision control (Yuan *et al*. 2008; Li *et al*. 2010). The testing steps and calibration methods used are described by Wu *et al*. (2006) and Guo *et al*. (2012).

4. Analytical results

4.a. Zircon U–Pb ages

The zircon U–Pb results are provided in online Supplementary Table S1 (available at http://journals.cambridge.org/geo). Zircon grains are grey, subhedral to euhedral, 50–150 μm long and with aspect ratios of 1:1 to 2:1. Zircons from samples Yd2006, Yd2009 and Yd2010 all display typical oscillatory zoning in cathodoluminescence (CL) images, whereas no obvious oscillatory zoning was observed in zircons from sample Yd2005 (Fig. 4). Zircons from sample Yd2005 show variable Th (7–778 ppm) and U (51–303 ppm) contents, and Th/U ratios of 0.11–2.57. A total of 23 concordant analyses yielded a $^{206}Pb/^{238}U$ weighted mean age of 123.3 ± 1.6 Ma (Fig. 5a). Eighteen zircons from sample Yd2006 have Th content of
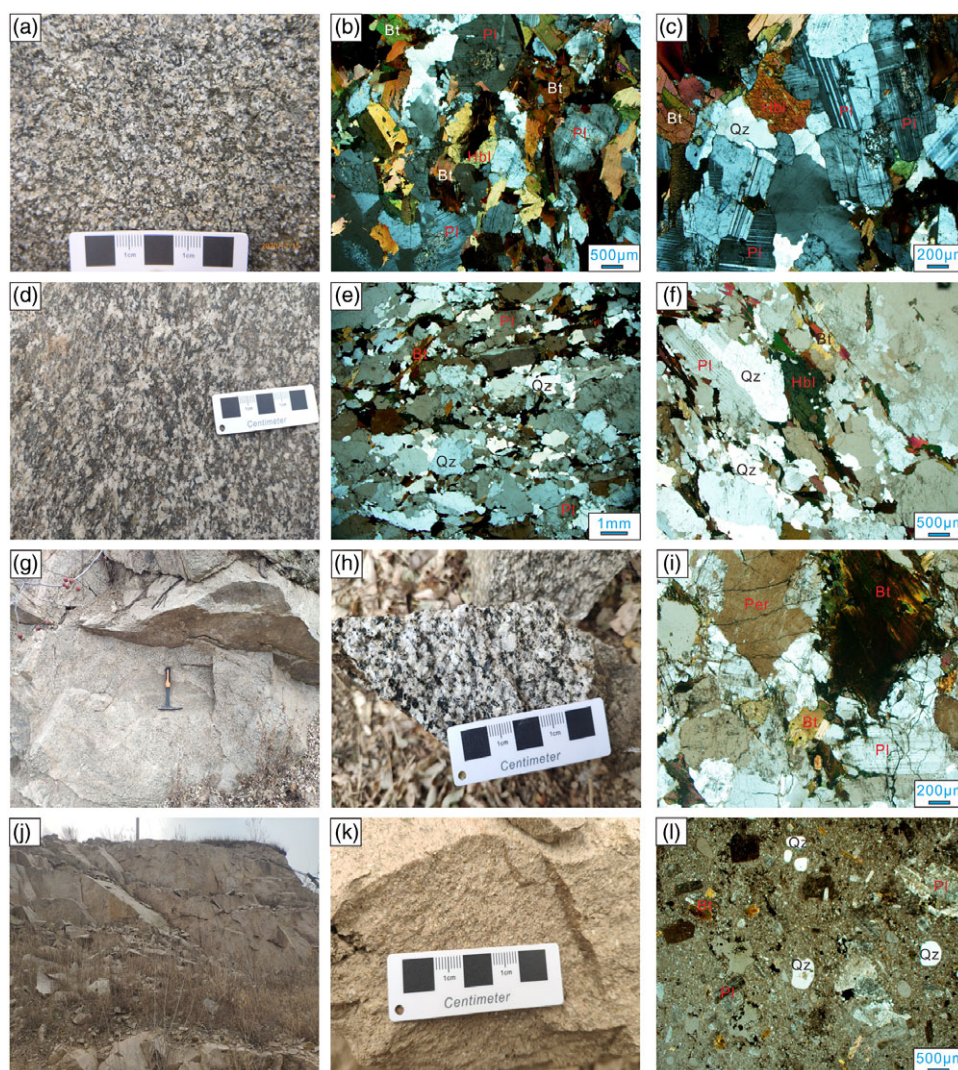
Fig. 3. (Colour online) Hand specimens and crossed-polarized light micrographs of rocks from Liaodong Peninsula from (a–c) monzodiorite (sample Yd2005); (d–f) granodiorite (sample Yd2006); (g–i) granodiorite (sample Yd2010); and (j–l) porphyritic monzogranite (sample Yd2009). Hbl – hornblende; Bt – biotite; Per – perthite; Pl – plagioclase; Qz – quartz.

67–346 ppm, U content of 48–266 ppm and Th/U ratios of 0.71–1.44, and yielded a $^{206}Pb/^{238}U$ weighted mean age of 125.5 ± 1.5 Ma (Fig. 5b). Sixteen zircons from sample Yd2009 display Th content of 68–690 ppm, U content of 115–410 ppm and Th/U ratios of 0.34–2.07, giving a mean age of 120.0 ± 1.9 Ma (Fig. 5c). Twenty concordant zircon analyses from sample Yd2010 yielded Th content of 166–760 ppm, U contents of 194–463 ppm and Th/U ratios of 0.72–1.34, with a mean age of 127.1 ± 1.2 Ma (Fig. 5d). Their ages range from 127–120 Ma, suggesting that they were formed during the Early Cretaceous Epoch. All zircons have high Th/U ratios (> 0.1), suggesting a magmatic origin (Hoskin & Schaltegger, 2003).

4.b. Major- and trace-element geochemistry

The major- and trace-element composition results are provided in online Supplementary Table S2. All samples have low loss on ignition (LOI; 0.29–1.11 wt%). Sample Yd2005 has low SiO_2 contents (55.93–56.16 wt%), high MgO contents (3.63–4.13 wt%) and high Al_2O_3 contents (16.78–17.58 wt%), giving Mg no. values of 48.24–50.77. Its K_2O and Na_2O contents are 2.48–2.58 wt% and 3.55–3.77 wt%, respectively, with low K_2O/Na_2O ratios (0.69–0.70). The samples demonstrate high-K and subalkaline features (Fig. 6a, b).

In contrast, samples Yd2006, Yd2009 and Yd2010 show high SiO_2 (63.77–70.80 wt%), high Al_2O_3 (14.13–17.38 wt%) and low MgO (0.36–1.78 wt%) contents, with Mg no. values of 21.18–46.83. Their K_2O and Na_2O contents are 2.05–5.37 wt% and 4.08–4.51 wt%, respectively, with variable K_2O/Na_2O ratios (0.45–1.31). The K_2O contents of these Pulandian plutons show positive correlation with the SiO_2 contents (Fig. 6b), whereas $Fe_2O_3^T$, TiO_2, P_2O_5, MgO, CaO and Al_2O_3 contents display negative correlations (Fig. 7a–f). The granodiorite (samples Yd2006 and Yd2010) shows high-K and subalkaline characteristics, whereas the porphyritic monzogranite (sample Yd2009) demonstrates shoshonitic and alkaline properties (Fig. 6a, b).

Samples have total rare earth element (REE) contents of 74–190 ppm and show enrichment in low REE (LREE) with high $(La/Yb)_N$ ratios (13.5–57.5). They have low Yb contents (0.54–1.24 ppm), low Y contents (4.9–16.4 ppm), high Sr contents (294–711 ppm; with the exception of one sample with 188 ppm content) and Sr/Y ratios of 38.5–108. In the chondrite-normalized REE pattern (Fig. 8), they display no clear Eu anomalies (Eu/Eu* = 0.79–1.21). The primitive-mantle-normalized spidergram (Fig. 8) reveals that these samples are enriched in large-ion lithophile elements (LILEs; e.g. Ba, K, Pb and Sr) and depleted in high-field-strength elements (HFSEs; e.g. Nb, Ta, P and Ti).
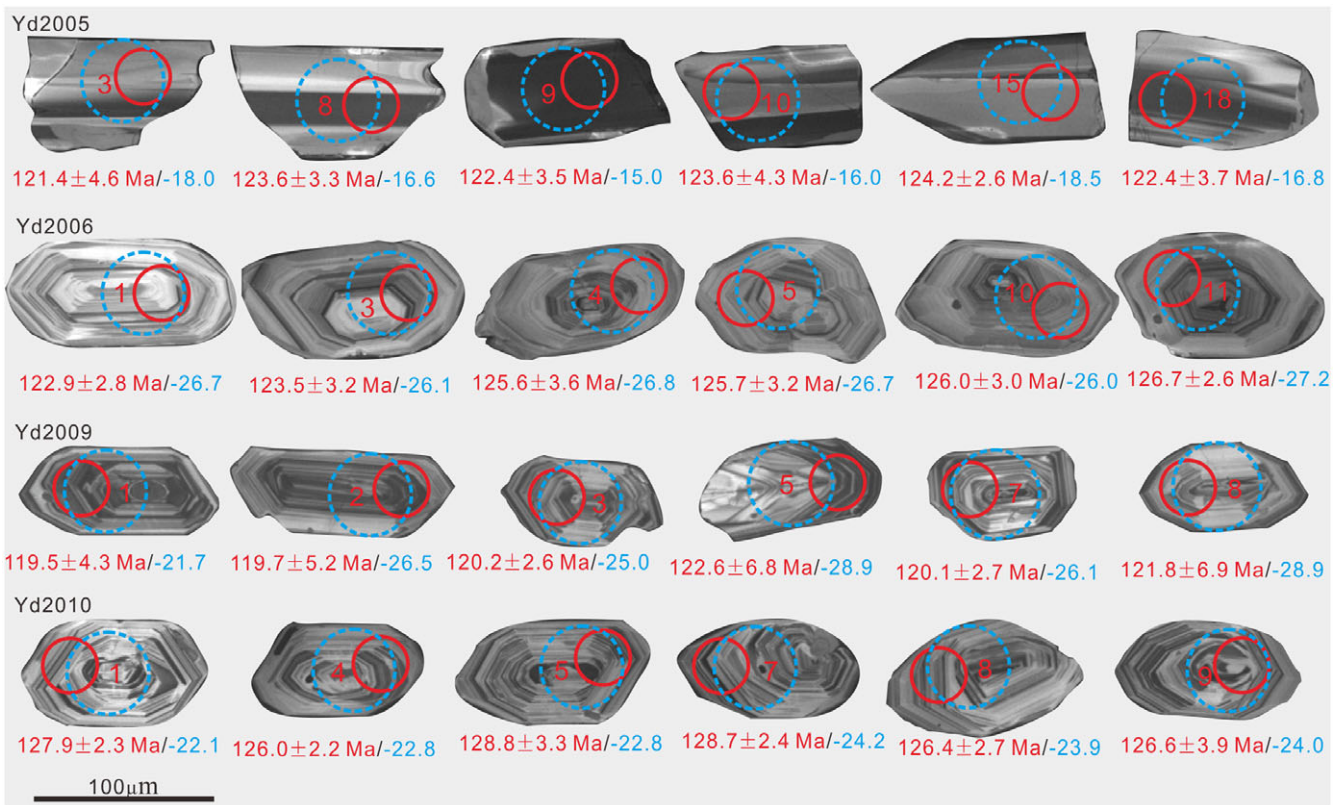
Fig. 4. (Colour online) Representative CL images of zircons from the samples. Solid red circles and blue circles indicate the locations of *in situ* U–Pb and Hf analyses spot, respectively.

4.c. Zircon Hf isotopic compositions

The results of the zircon Hf isotopic analysis are provided in online Supplementary Table S3. Sample Yd2005 yielded relatively uniform $^{176}Hf/^{177}Hf$ ratios of 0.282275 to 0.282176, with $\epsilon_{Hf}(t)$ values of −18.5 to −15.0 and two-stage model ages (T_{DM2}) of 2351–2131 Ma. Sample Yd2006 zircon $\epsilon_{Hf}(t)$ values ranged from −27.2 to −25.4, with $^{176}Hf/^{177}Hf$ ratios of 0.281977–0.281927 and T_{DM2} ages of 2899–2789 Ma. Sample Yd2009 yielded zircon $\epsilon_{Hf}(t)$ values ranging from −28.9 to −21.1, with $^{176}Hf/^{177}Hf$ ratios of 0.282107–0.281882 and T_{DM2} ages of 3004–2511 Ma. The $\epsilon_{Hf}(t)$ values of sample Yd2010 ranged from −24.6 to −22.1, and its corresponding $^{176}Hf/^{177}Hf$ ratios and T_{DM2} ages ranged over 0.282071–0.282000 and 2937–2580 Ma.

5. Discussion

5.a. Rock type and petrogenesis

Although the samples yielded very low LOI (0.29–1.11 wt%), the effect of element migration must be excluded before the geochemical characteristics of the rocks can be interpreted. Studies have shown that the major elements, HFSEs and REEs can remain constant during weak alteration, whereas LILEs can migrate more easily (Alirezaei & Cameron 2002); LILEs are therefore good indicators to gauge the effect of weak alteration on the samples. Some ratios (e.g. K/Sr and La/Th) can be used to monitor the mobility of the LILEs (Rudnick *et al.* 1985). All sample have low to medium K/Sr ratios (26–233) and low La/Th ratios (3.0–7.1), suggesting that the weak alteration did not modify their element compositions (Xin *et al.* 2019). The geochemical data of the

selected samples, such as major- and trace-element content, therefore reflects their inherited magmatic source characteristics.

All samples in this study are characterized by high Sr contents (294–711 ppm), high Al_2O_3 contents (14.13–17.58 wt%), high Sr/Y ratios (38.5–108), low Yb contents (0.54–1.24 ppm), low Y contents (4.9–16.4 ppm) and no clear Eu anomalies (Eu/Eu* = 0.79–1.21), displaying typical adakitic geochemical characteristics (Defant & Drummond, 1990). In addition, most samples fall within the classification of adakite (Fig. 9a, b). These rocks have K_2O/Na_2O ratios (0.48–1.31) higher than for those of typical adakitic rocks (*c.* 0.4; Moyen, 2009), which are similar to K-rich adakites from Dabie orogen (Fig. 10a; Wang *et al.* 2007). The trace-element pattern of the rocks is also similar to that for the K-rich adakite rocks (Fig. 8); the samples can therefore be identified as K-rich adakitic rocks.

Adakites are formed during various tectonomagmatic processes, such as partial melting of subducted oceanic slab (Defant & Drummond, 1990; Wang *et al.* 2007); AFC associated with basaltic magmas (Wareham *et al.* 1997; Castillo *et al.* 1999); magma mixing of basaltic magmas and crustal-derived felsic magmas (Guo *et al.* 2007; Xu *et al.* 2012); partial melting of thickened lower continental crust (Atherton & Petford, 1993; Petford & Atherton, 1996; Wang *et al.* 2005); and partial melting of delaminated lower continental crust (Gao *et al.* 2004; Hou *et al.* 2004).

Adakitic rocks were originally defined as the partial melting of subducted young, hot slabs (Defant & Drummond, 1990). As the slab melt rises, it is metasomatized by mantle-derived material, resulting in rocks characterized by low K_2O/Na_2O ratios (*c.* 0.5) and high MgO (*c.* 4–9 wt%), Mg no. (> 50), Ni and Cr contents (Stern & Kilian, 1996). The Pulandian adakitic rocks have high

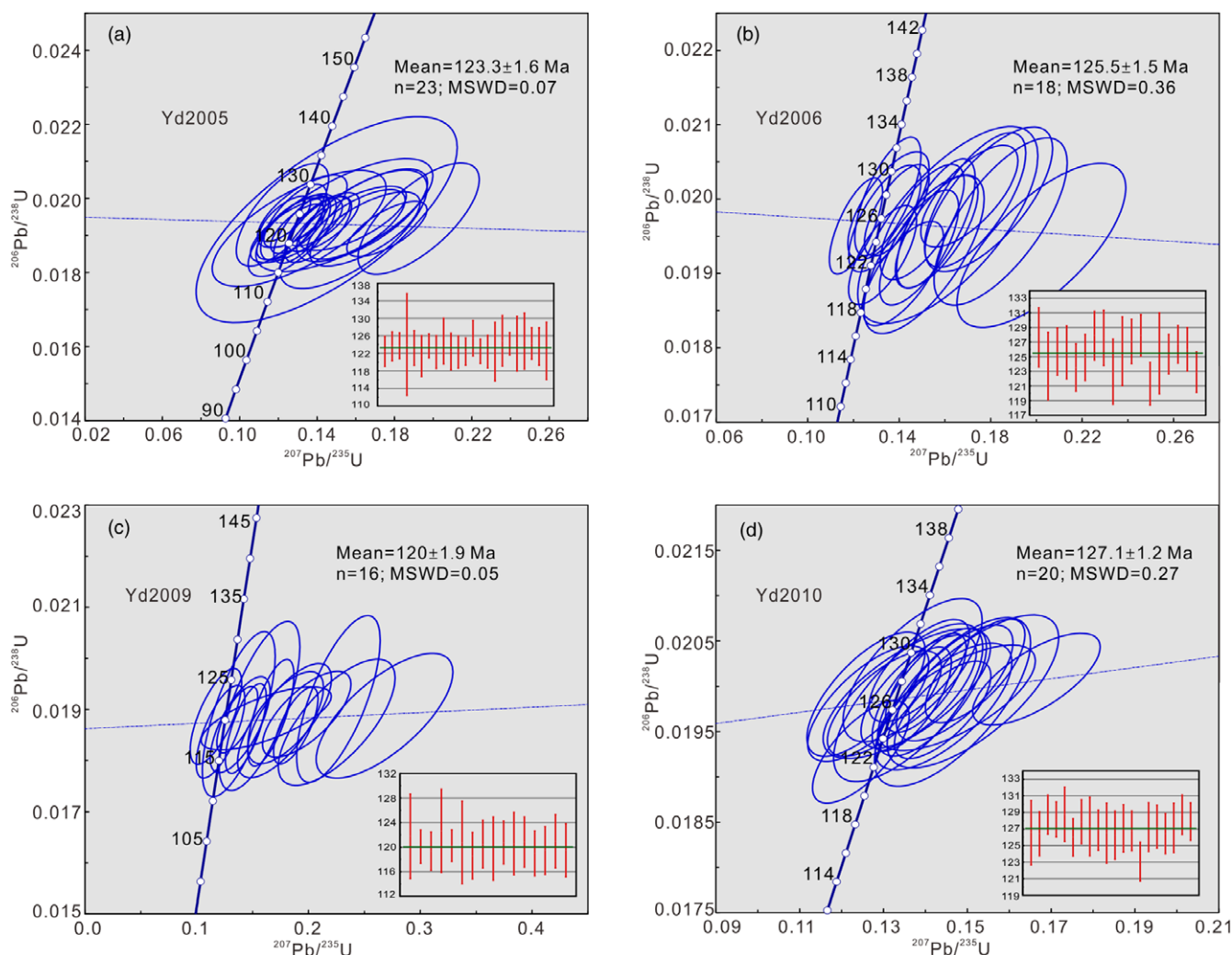**Fig. 5.** (Colour online) Zircon U–Pb concordia and weighted mean diagrams of the Pulandian samples.
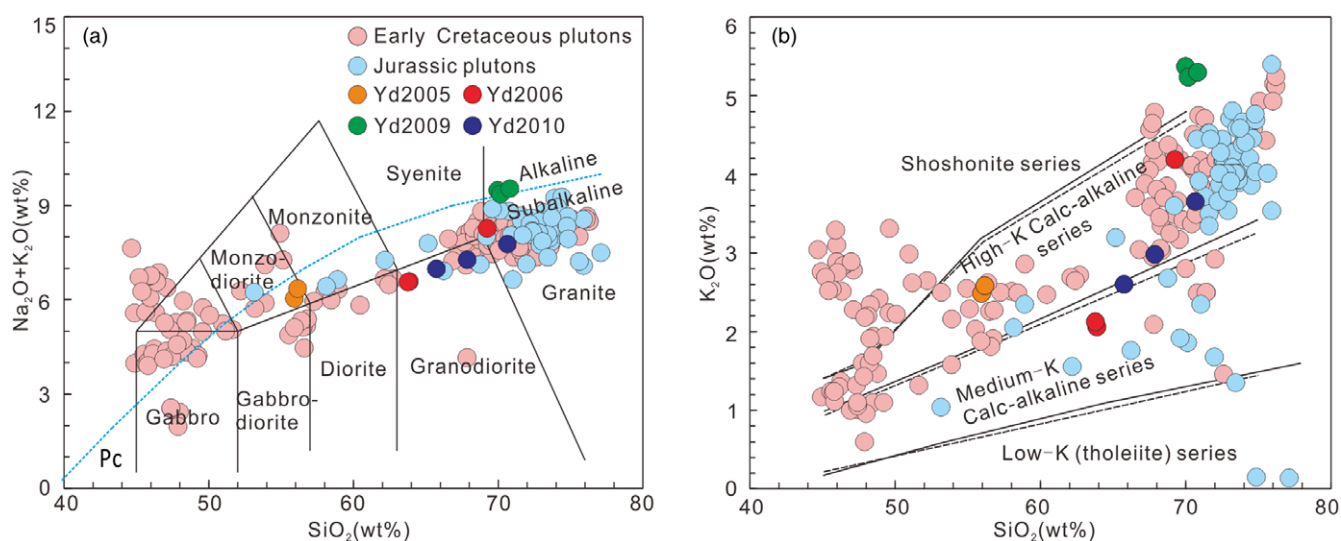

Fig. 6. (Colour online) (a) SiO$_2$ and K$_2$O + Na$_2$O correlation (TAS) diagram (after Wilson, 1989); and (b) SiO$_2$ and K$_2$O correlation diagram (after Peccerillo & Taylor, 1976). Data from Wu *et al.* (2005*a*, *b*); Wang *et al.* (2007); Yang *et al.* (2007*a*, *b*).
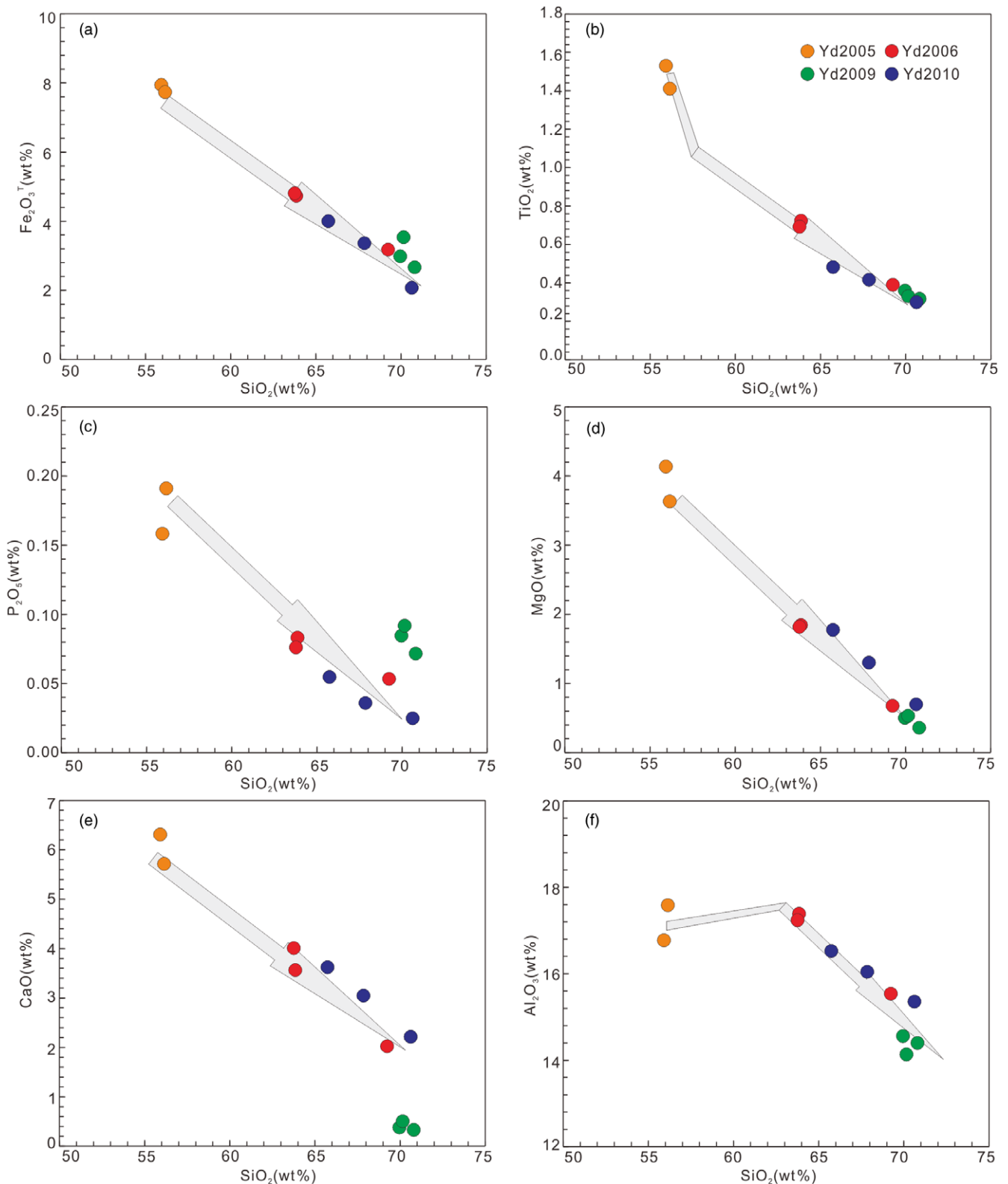
Fig. 7. (Colour online) Harker diagrams display the major-element variations of the Pulandian plutons.

K_2O/Na_2O ratios (mean 0.85) and low MgO content (0.36–4.13 wt %), Mg no. (mean 37.7), Ni content (mean 20 ppm) and Cr content (mean 44 ppm), which are inconsistent with the features of melt of subducted oceanic slab. The samples have low Ce/Pb ratios (mean 7.6) and obvious negative Nb and Ta anomalies (Fig. 7), indicating that they may have originated in continental crustal source rather than partial melting or AFC of oceanic basalts (Ce/Pb > 20) (Rudnick & Fountain, 1995; Plank, 2005). Moreover, no clear
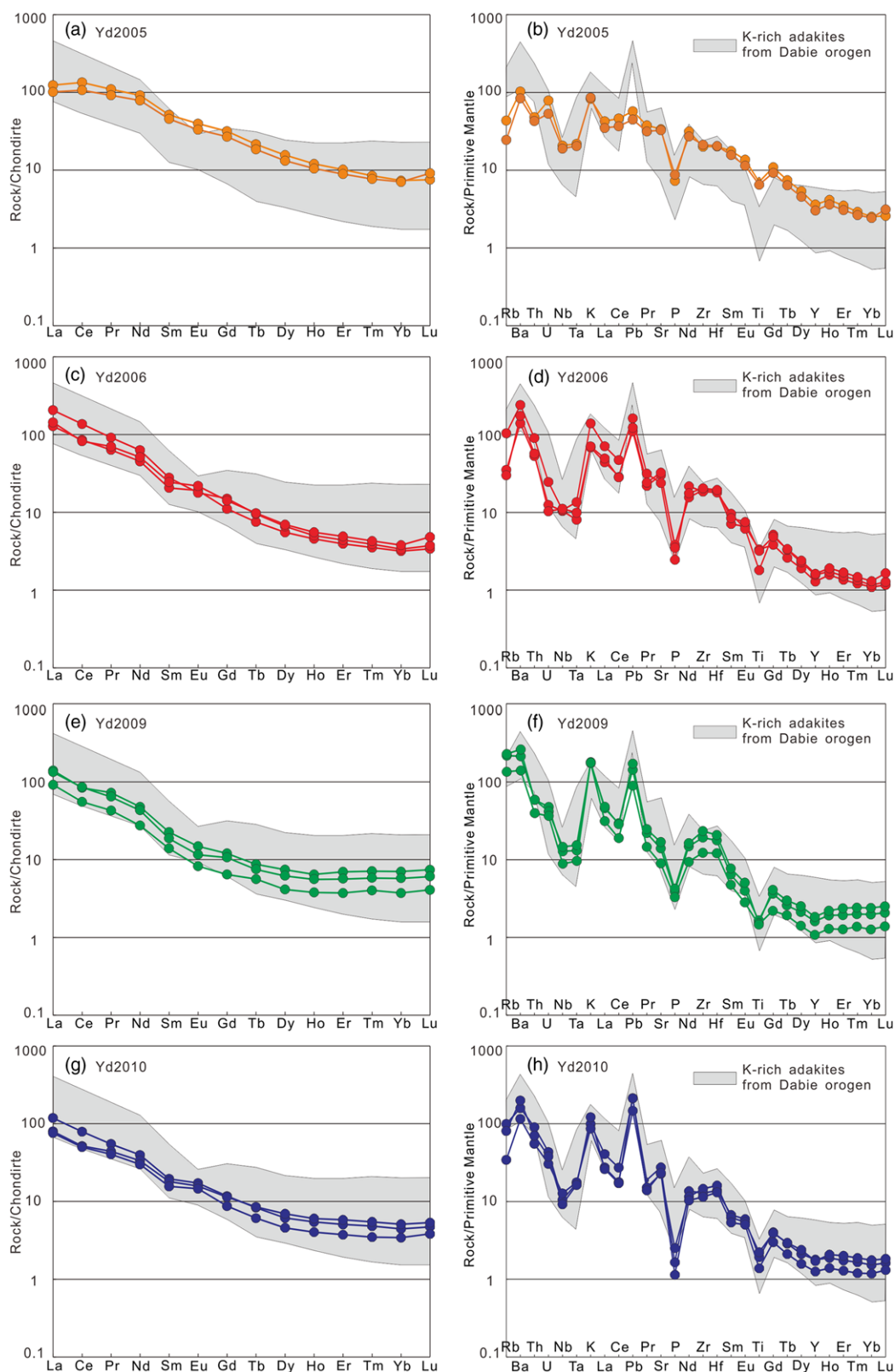
Fig. 8. (Colour online) Chondrite-normalized REE and primitive-mantle-normalized trace-element patterns for the samples. Normalized data for normalization and plotting after Sun & McDonough (1989). K-rich adakites data from Wang *et al.* (2007).

Eu anomalies in all the samples imply that fractional crystallization of plagioclase did not play a crucial role in the process of their formation (Wang *et al.* 2007). The lack of obvious indications of fractional crystallization (Fig. 10b) and of large-scale mafic rocks

around Pulandian area (Fig. 2) also support the fact that these rocks were not formed from AFC of basalt. The significant negative $\epsilon_{Hf}(t)$ values (-33.3 to -15.0) indicate that they derived from partial melting of the ancient crust rather than magmatic mixing
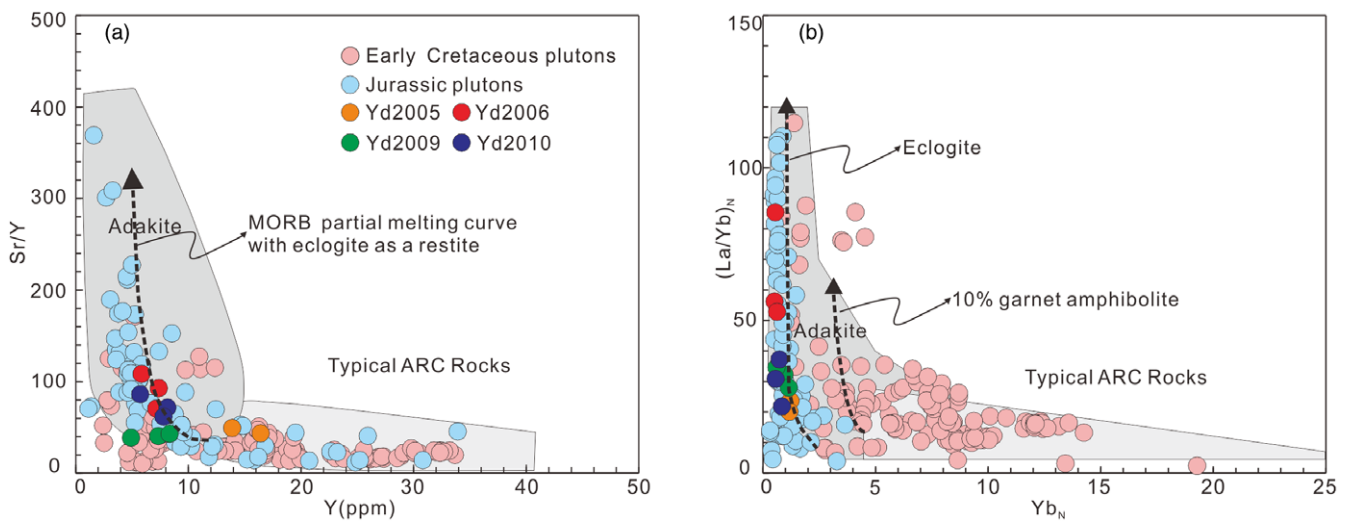
Fig. 9. (Colour online) (a) Sr/Y versus Y diagram (after Defant *et al*. 2002); and (b) (La/Yb)$_N$ versus Yb$_N$ diagram (after Martin, 1999). Data from Zhang & Wan (2001) and Xiong *et al*. (2011).
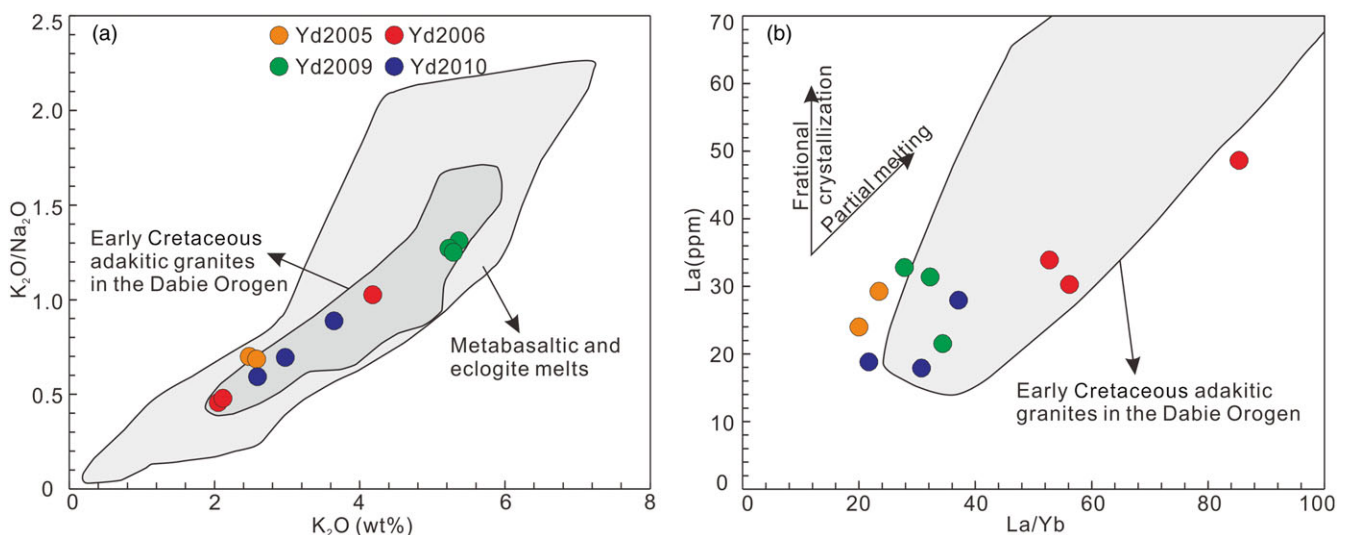

Fig. 10. (Colour online) (a) K$_2$O/Na$_2$O versus K$_2$O and (b) La/Yb versus La (after Wang *et al*. 2007).

(Fig. 11a). The geochemical characteristics of the samples are similar and there are no mafic microgranular enclaves in the rocks (Figs 3, 6, 8); magma mixing therefore does not explain their origin. The melt formed by partial melting of the delaminated lower crust may have been upwelling, resulting in interaction with the mantle and the production of geochemical features similar to those of the melting of the subducted oceanic slab (Xu *et al.* 2012); the rocks therefore did not originate from the partial melting of the delaminated lower crust. Experimental petrology shows that adakitic magmas can be formed by partial melting of the thickened lower continental crust (Petford & Atherton, 1996; Xiong *et al.* 2005). The melts from the above model are characterized by low MgO (< 2 wt%) and Mg no. (< 50), and high SiO$_2$ (> 60 wt%) and K$_2$O (> 2 wt%) contents, which are matched by the features of all samples (see online Supplementary Table S2). As shown in TiO$_2$ versus SiO$_2$ and MgO versus SiO$_2$ diagrams (Fig. 12), the

majority of the samples from Pulandian plot within the field of thickened lower-crust-derived adakitic rocks.

Previous studies shown that while partial melting if the garnet is remained as residue, the partial melt result HREE depletion (Othman *et al.* 1989; Wang *et al.* 2007). Plagioclase has a large partition coefficient for Sr and Eu elements, and its crystallization can result in Sr and Eu negative anomalies (Nash & Crecraft, 1985). On the basis of the geochemical features (online Supplementary Table S2; Fig. 8), the residues are rich in garnet and poor in plagioclase. According to partial melting experimental research, garnet-absent and plagioclase-rich samples indicate formation pressures lower than 10 kbar, both garnet and plagioclase are present at formation pressures of 12.5–15 kbar, and garnet-rich and plagioclase-absent samples indicate formation pressures higher than 15 kbar (Skjerlie & Johnston, 1993; Sen & Dunn, 1994; Patiño Douce & Beard, 1995; Litvinovsky *et al.* 2000). The
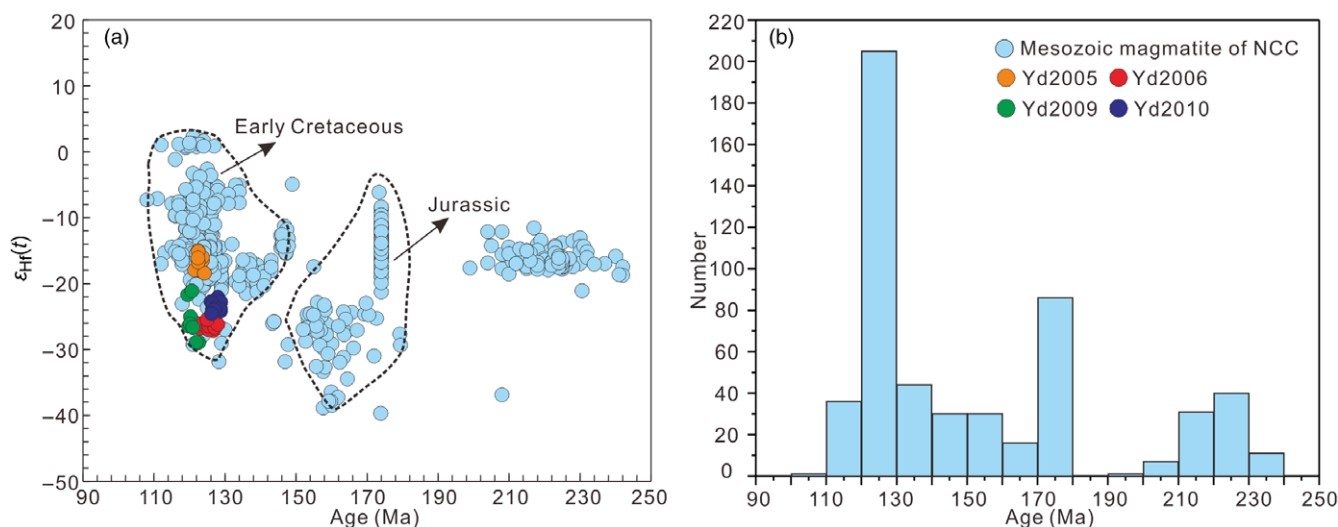
Fig. 11. (Colour online) (a) $\epsilon_{Hf}(t)$ versus age (Ma) and (b) age histogram of Mesozoic magmatic rocks of NCC. Data from Yang *et al.* (2004, 2007*a*, *b*).

above-mentioned residues can therefore only form in a high-pressure environment, in accordance with the pressure of thickened lower continental crust. The source and petrogenesis of the Pulandian plutons can be further illustrated with diagrams discerning the source nature of adakites (Foley *et al.* 2002). In the K_2O versus K_2O/Na_2O diagram (Fig. 10a), samples fall within the metabasaltic and eclogite melt fields, similar to the adakitic granites in the Dabie Orogen. In the $(La/Yb)_N$ versus Yb_N diagram (Fig. 9b), all plots are mainly close to the melt of eclogite. We therefore suggest that the Pulandian adakitic rocks were formed by partial melting of thickened eclogitic lower crust.

5.b. Tectonic setting and geodynamic mechanism

Magmatic and volcanic activities were strong in the Liaoning Peninsula during the Early Cretaceous Epoch, which resulted in the formation of numerous intrusive rocks (Fig. 1b). The lithology of magmatic rocks in this period is mainly monzogranite, granodiorite and alkaline granite (Yang *et al.* 2004; Liu *et al.* 2019). According to the results of previous research, some Early Cretaceous A-type granites and alkaline rocks have been reported in the Liaoning Peninsula – for example, Qianshan granite (127 Ma), Taipingshan alkaline feldspar granite (129 Ma), Guanmenshan Granite porphyry (126 Ma) and quartz syenite (127 Ma) – which indicate that the Liaodong Peninsula existed in an extensional tectonic setting (Yang *et al.* 2007*a*, *b*; Liu *et al.* 2016, 2019). Metamorphic core complexes (MCC) are also widely developed in the Liaoning Peninsula; for example, the Yinmawan (129–120 Ma) and Gudaoling (127–118 Ma) plutons were emplaced along the detachment fault of the Liaonan–Wanfu MCC (130–113 Ma), which was in an extensional tectonic environment (Guan *et al.* 2008; Ji, 2010). Zhu & Xu (2019) reported that the slab rollback of the Palaeo-Pacific Ocean began at *c.* 145 Ma, which may have resulted in the extension of the NCC. We therefore believe that the Early Cretaceous (130–120 Ma) extension was closely related to the slab rollback of the Palaeo-Pacific Ocean. The age of the Pulandian plutons is 127–120 Ma, which is nearly the same as the above pluton ages. The Pulandian plutons show LILE-enriched and HFSE-depleted characteristics, which indicate that these rocks were formed in a subduction environment. In the tectonic diagrams (Fig. 13), all samples fall within the area of

arc-related environment. Combined with age and features, we believe that they were formed in an extensional setting involved in slab rollback of the Palaeo-Pacific Ocean.

Previous studies on mantle xenoliths indicate that the thickness of the NCC was 200 km during the Palaeozoic Era and 80–100 km during the Cenozoic Era, suggesting that significant destruction and lithospheric thinning occurred (Fan *et al.* 2000; Wu *et al.* 2019). The constructed seismic data of the NCC also support dramatic thinning (Zhu *et al.* 2011). In recent years, there has been more progress in determining the dynamic setting of lithospheric thinning of NCC (Wu *et al.* 2005*a*; Zheng *et al.* 2007, 2018; Zhu *et al.* 2012; Niu *et al.* 2015). However, the geodynamic mechanism remains controversial and researchers are focused on two separate models: (1) rapid lithospheric delamination (e.g. Gao *et al.* 2004; Wu *et al.* 2005*b*, 2008); and (2) thermo-mechanical-chemical erosion (e.g. Griffin *et al.* 1998; Zheng *et al.* 2007). Frequent magmatic activity was one of the important forms of destruction of NCC; the Liaodong Peninsula is the strongest and most typical area of destruction (Liu *et al.* 2011). A fuller understanding of the magmatic rocks of the Liaodong Peninsula will therefore yield knowledge of the lithospheric thinning and destruction of NCC.

During the Jurassic Period, the intrusive rocks in Liaodong Peninsula were dominated by quartz diorite, granodiorite and monzogranite, etc., most of which belong to high-K calc-alkaline granite (Fig. 6b; Yang *et al.* 2004, 2007*a*, *b*; Wu *et al.* 2005*b*; Sun *et al.* 2005). There were also many Jurassic adakites (Fig. 9), derived from the partial melting of the thickened lower crust (Gao *et al.* 2004; Wu *et al.* 2005*b*; Zhu *et al.* 2012). In addition, the negative Lu–Hf isotopes also supported the theory that Jurassic granites are mainly derived from the partial melting of ancient thickened lower crust (Fig. 11a). The existence of thickened lower crust is the premise of lithospheric delamination. The rock types of Early Cretaceous intrusions in Liaodong Peninsula are complex, mainly composed of I-type granite, A-type granite, alkaline and mafic rock (Fig. 6; Sun & Yang, 2009; Lan *et al.* 2011). According to previous studies on geochemistry and Lu–Hf isotopes (−30 to +5; Fig. 11a), rocks from this period may have originated from different magma sources such as depleted mantle, enriched lithospheric mantle or ancient lower crust (Wu *et al.* 2019), possibly the result of intensive crust–mantle interaction caused by asthenosphere upwelling after lithospheric delamination
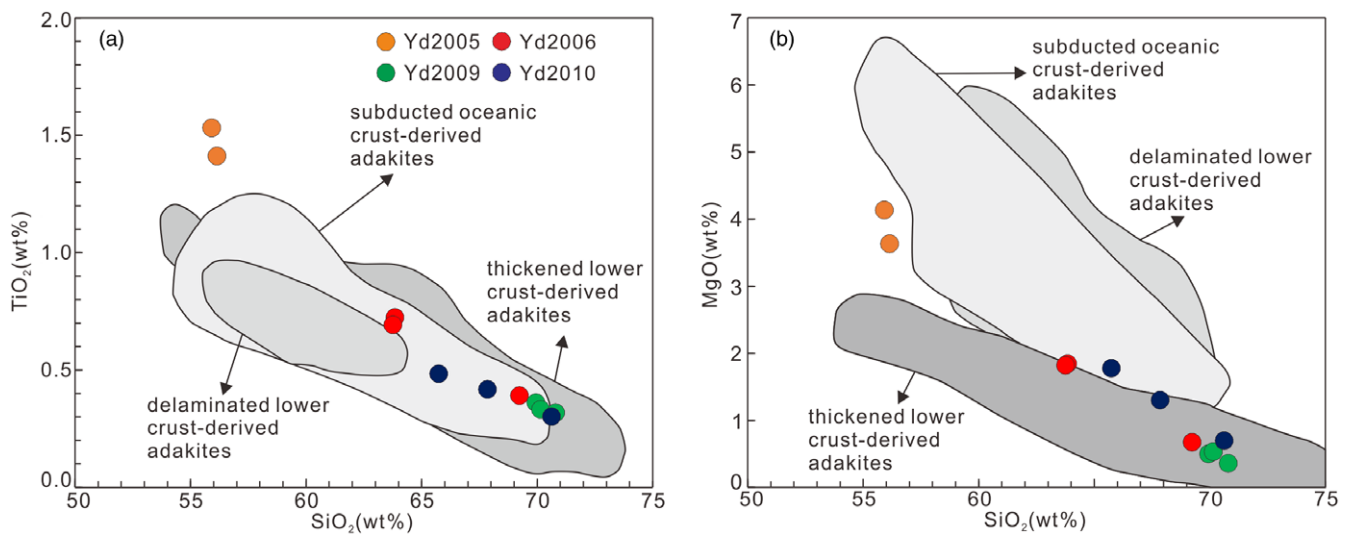
Fig. 12. (Colour online) (a) TiO₂ versus SiO₂ and (b) MgO versus SiO₂ diagrams for samples. The field of subducted oceanic crust-derived adakites are after Wang *et al*. (2007). The field of thickened lower crust-derived adakites are after Atherton & Petford (1993) and Muir *et al*. (1995), and the field of delaminated lower crust-derived adakities are after Wang *et al*. (2004*a, b*, 2007).
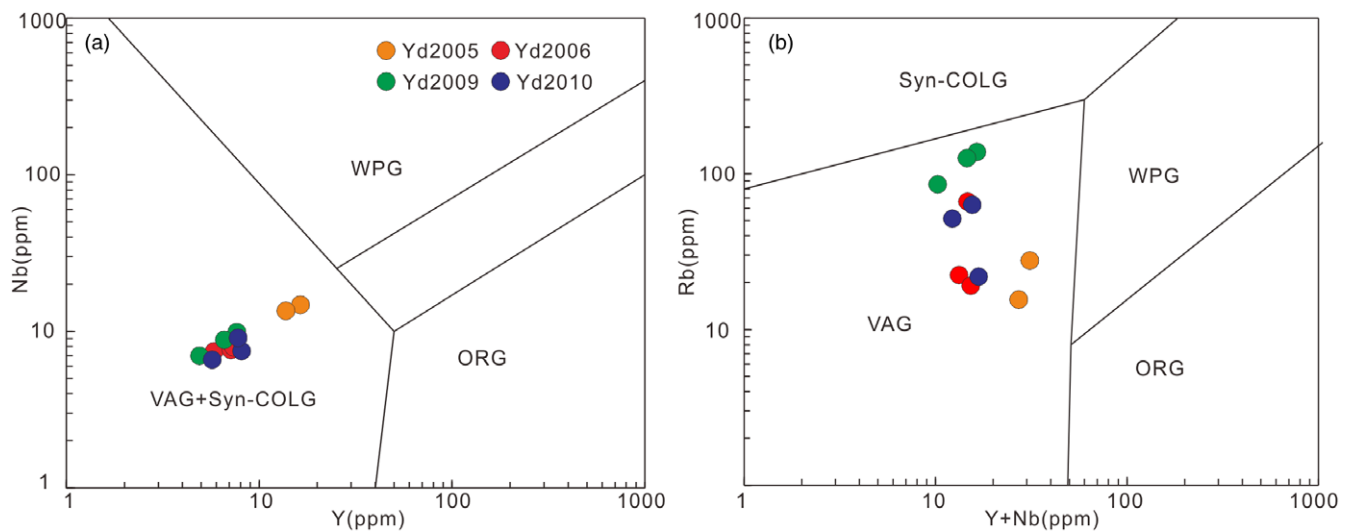

Fig. 13. (Colour online) (a) Y versus Nb and (b) (Y + Nb) versus Rb (Pearce *et al*. 1984) for Pulandian sample rocks. VAG – volcanic-arc granites; syn-COLG – syn-collisional granites; ORG – orogenic ridge granites; WPG – within-plate granites.

of the NCC. The wide distribution of magmatic rocks (Fig. 11b) and extensional tectonics over a short period (*c*. 130–120 Ma) in the Liaodong Peninsula (Liu *et al.* 2005) is consistent with the rapid lithospheric delamination characteristics. We therefore suggest that the lithospheric delamination model is a better geodynamic mechanism for the thinning and destruction of the NCC than thermo-mechanical-chemical erosion.

Several possible trigger factors for lithospheric delamination have recently been proposed, including: (1) thickened lower crust (Gao *et al.* 2004, 2009); (2) hydrous fluids or melts related to Palaeo-Pacific subduction (Gao *et al.* 2009; Zhu *et al.* 2011; Zhu & Xu, 2019); and (3) upwelling asthenosphere (Deng *et al.* 2007; Liu *et al.* 2020). First, thickened lower crust is a crucial precondition to lithosphere delamination. The thickened lower crust undergoes a phase transformation of the eclogite, which makes it denser than the lithospheric mantle (Kay & Kay, 1993). The Jurassic subduction of the Palaeo-Pacific Ocean caused the crust

of the NCC to thicken (Fig. 14a; Wu *et al.* 2005*b*; Zhu & Xu, 2019). The Jurassic and Early Cretaceous adakites in the Liaodong Peninsula provide evidence for the thickened crust of the NCC (Yang *et al.* 2004; Wu *et al.* 2005*b*; Zhang *et al.* 2010; this study). The thickened crust (eclogitic layer) could not directly sink because of the refractory and buoyant nature of the NCC lithospheric mantle (Deng *et al.* 2007). Secondly, the lithospheric mantle was metasomatized by hydrous fluids or melt produced by the subduction of the Palaeo-Pacific subduction (Niu *et al.* 2015). At *c.* 145 Ma the Palaeo-Pacific Ocean started to rollback, resulting in asthenosphere upwelling (Fig. 14b; Zheng *et al.* 2018; Zhu & Xu, 2019). At *c.* 130–120 Ma, the Palaeo-Pacific Ocean reached its maximum rate of subduction slab rollback, transitioned into a high-angle subduction and produced a stagnation slab in the mantle zone (Fig. 14c; Zhu & Xu, 2019). Because of the slower slab rollback and weak asthenosphere upwelling at 145 Ma, we believe that the refractory and thick lithospheric mantle of the NCC
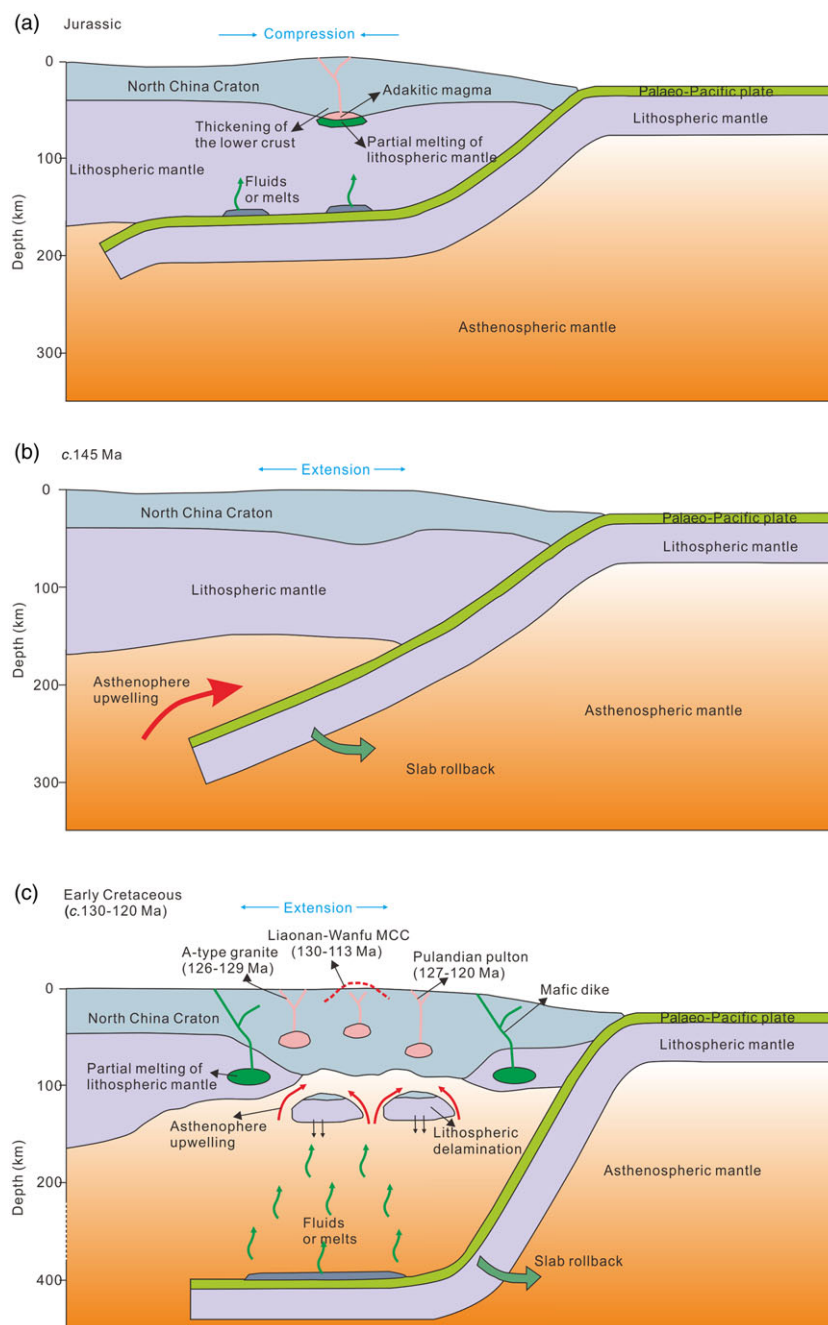
Fig. 14. (Colour online) Lithospheric evolution process of the NCC during the Mesozoic Era. (a) Jurassic: the Palaeo-Pacific Ocean subducted, causing the NCC crust to thicken (Wu *et al.* 2005*b*). (b) *c.* 145 Ma: the subducting Palaeo-Pacific slab began to rollback with the asthenosphere upwelling (Zhu & Xu, 2019). (C) Early Cretaceous (*c.* 130–120 Ma): the Palaeo-Pacific Ocean reached its maximum rate of subduction slab rollback, transitioned into a high-angle subduction and produced a stagnation slab in the mantle zone. The stagnation slab began to dehydrate, changing the physical properties of the overlying lithospheric mantle, which caused its stability to be disrupted and its subsequent delamination. During the period, widespread extensional tectonics occurred in the shallow crust of the NCC. The Liaonan–Wanfu MCC and rocks of different types and properties were generated (e.g. I-/A-type granite, adakites rock; Yang *et al.* 2004; Wu *et al.* 2005*b*; this study). MCC – metamorphic core complexes.

experienced a small-scale partial melting (Zheng *et al.* 2016, 2018). At *c.* 130–120 Ma, the stagnation slab began to dehydrate, changing the physical properties of the overlying lithospheric mantle (e.g. decreasing its viscosity) and causing its stability to be disrupted (Zhu *et al.* 2011). Under the combined action of these processes, the lithosphere of the NCC underwent delamination. This resulted in a rapid upwelling of large amounts of asthenosphere, providing more heat and accelerating partial melting of the lithospheric mantle. During this period, a large number of rocks of different sources and properties were generated (e.g. I-/A-type granite, adakites and rock; Yang *et al.* 2004; Wu *et al.* 2005*b*; this study). Meanwhile, the widespread extensional tectonics and metamorphic core complexes appear during this stage.

6. Conclusions

(1) The Pulandian monzodiorite, granodiorite and porphyritic monzogranite are adakitic rocks that were emplaced at 127–120 Ma (i.e. Early Cretaceous).

(2) The Pulandian adakitic rocks were formed by partial melting of thickened eclogitic lower crust, and in an extensional setting related to slab rollback of the Palaeo-Pacific Ocean.

(3) As a result of the rapid slab rollback of the Palaeo-Pacific Ocean during *c.* 130–120 Ma, the asthenosphere upwelled and modified the thickened lithospheric mantle, which lost its stability, eventually resulting in the lithospheric delamination and thinning of the NCC.

References

Alirezaei S and Cameron EM (2002) Mass balance during gabbro-amphibolite transition, Bamble Sector, Norway: Implications for petrogenesis and tectonic setting of the gabbros. *Lithos* **60**, 21–45. doi: 10.1016/S0024-4937(01)00076-7

Andersen T (2002) Correction of common lead in U-Pb analyses that do not report ^{204}Pb. *Chemical Geology* **192**, 59–79. doi: 10.1016/S0009-2541(02)00195-X

Atherton MP and Petford N (1993) Generation of sodium-rich magmas from newly underplated basaltic crust. *Nature* **36**, 144–6. doi: 10.1038/362144a0

Castillo PR, Janney PE and Solidum RU (1999) Petrology and geochemistry of Camiguin Island, southern Philippines: Insights to the source of adakites and other lavas in a complex arc setting. *Contributions to Mineralogy and Petrology* **134**, 33–51. doi: 10.1007/s004100050467

Defant MJ and Drummond MS (1990) Derivation of some modern arc magmas by melting of young subducted lithosphere. *Nature* **347**, 662–5. doi: 10.1038/347662a0

Defant MJ, Xu JF, Kepezhinskas P, Wang Q, Zhang Q and Xiao L (2002) Adakites: some variations on a theme. *Acta Petrologica Sinica* **18**, 129–42. doi: 10.1007/s10958-012-0719-1

Deng J, Su S, Niu Y, Liu C, Zhao GC, Zhao XG, Zhou S and Wu ZX (2007) A possible model for the lithospheric thinning of North China Craton: evidence from the Yanshanian (Jura-Cretaceous) magmatism and tectonism. *Lithos* **96**, 22–35. doi: 10.1016/j.lithos.2006.09.009

Deng JF, Mo X and Zhao H (1994) Lithosphere root/de-rooting and activation of the east China continent. *Geoscience* **8**, 349–56 (in Chinese with English abstract).

Duan X, Zeng Q, Yang J, Liu JM, Wang YB and Zhou LL (2014) Geochronology, geochemistry and Hf isotope of Late Triassic magmatic rocks of Qingchengzi district in Liaodong peninsula, Northeast China. *Journal of Asian Earth Sciences* **91**, 107–24. doi: 10.1016/j.jseaes.2014.05.009

Fan WM, Zhang HF, Baker J, Jarvis KE, Mason PRD and Menzies MA (2000) On and off the North China Craton: where is the Archaean keel? *Journal of Petrology* **41**, 933–50. doi: 10.1093/petrology/41.7.933

Foley S, Tiepolo M and Vannucci R (2002) Growth of early continental crust controlled by melting of amphibolite in subduction zones. *Nature* **417**, 837–40. doi: 10.1038/nature00799

Gao S, Rudnick RL, Carlson RW, McDonough WF and Liu YS (2002) Re-Os evidence for replacement of ancient mantle lithosphere beneath the North China craton. *Earth & Planetary Science Letters* **198**, 307–22. doi: 10.1016/S0012-821X(02)00489-2

Gao S, Rudnick RL, Yuan HL, Liu XM, Liu YS, Xu WL, Ling WL, Ayers J, Wang XC and Wang QH (2004) Recycling lower continental crust in the North China craton. *Nature* **432**, 892–97. doi: 10.1038/nature03162

Gao S, Zhang JF, Xu WL and Liu YS (2009) Delamination and destruction of the North China Craton. *Chinese Science Bulletin* **54**, 3367–78. doi: CNKI:SUN:JXTW.0.2009-19-005

Griffin WL, Zhang AD, O'Reilly SY and Ryan CG (1998) Phanerozoic evolution of the lithosphere beneath the Sino-Korean craton. *Geodynamics Series* **27**, 107–26.

Guan SH, Liu JL, Ji M, Zhao JS, Hu L and Gregory AD (2008) Discovery of the Wanfu metamorphic core complex in southern Liaoning and its regional tectonic implication. *Earth Science Frontiers* **15**, 199–208. doi: 10.3321/j.issn:1005-2321.2008.03.016

Guo C, Chen Y, Zeng Z and Lou F (2012) Petrogenesis of the Xihuashan granites in southeastern China: constraints from geochemistry and in-situ analyses of zircon U-Pb-Hf-O isotopes. *Lithos* **148**, 209–27. doi: 10.1016/j.lithos.2012.06.014

Guo F, Fan W and Li C (2006) Geochemistry of late Mesozoic adakites from the Sulu belt, eastern China: Magma genesis and implications for crustal recycling beneath continental collisional orogens. *Geological Magazine* **143**, 1–13. doi: 10.1017/S0016756805001214

Guo F, Nakamuru E, Fan W, Kobayoshi K and Li CW (2007) Generation of Paleocene adakitic andesites by magma mixing; Yanji Area, NE China. *Journal of Petrology* **48**, 661–92. doi: 10.1093/petrology/egl077

Hoskin PWO and Schaltegger U (2003) The composition of zircon and igneous and metamorphic petrogenesis. *Reviews in Mineralogy and Geochemistry* **53**, 27–62. doi: 10.2113/0530027

Hou ZQ, Gao YF, Qu XM, Rui ZY and Mo XX (2004) Origin of adakitic intrusives generated during mid-Miocene east-west extension in southern Tibet. *Earth and Planetary Science Letters* **220**, 139–55. doi: 10.1016/S0012-821X(04)00007-X

Ji M (2010) Early Cretaceous tectono-magmatic processes in the Liaodong Peninsula and regional tectonic implications. Ph.D. thesis. Chinese University of Geoscience, Beijing (in Chinese with English abstract). Published thesis.

Jiang YH, Jiang SY, Ling HF and Ni P (2010) Petrogenesis and tectonic implications of late Jurassic shoshonitic lamprophyre dikes from the Liaodong Peninsula, NE China. *Mineralogy and Petrology* **100**, 127–51. doi: 10.1007/s00710-010-0124-8

Kay RW and Kay SM (1993) Delamination and delamination magmatism. *Tectonophysics* **219**, 177–89. doi: 10.1016/0040-1951(93)90295-U

Lan TG, Fan HR, Hu FF, Tomkins AG, Yang KF and Liu Y (2011) Multiple crust-mantle interactions for the destruction of the North China Craton: geochemical and Sr-Nd-Pb-Hf isotopic evidence from the Longbaoshan alkaline complex. *Lithos* **183**, 695–705. doi: 10.1016/j.lithos.2010.12.001

Li XH, Long WG, Li QL, Liu Y, Zheng YF, Yang YH, Chamberlain KR, Wan DF, Guo CH, Wang XC and Tao H (2010) Penglai zircon megacrysts: a potential new working reference material for microbeam determination of Hf-O isotopes and U-Pb age. *Geostandards and Geoanalytical Research* **34**, 117–34. doi: 10.1111/j.1751-908X.2010.00036.x

Li XS (2019) The petrogenesis and tectonic setting of the Early Cretaceous basic dikes in Pulandian area, Liaodong Peninsula. M.Sc. Chinese University of Geoscience, Beijing (in Chinese with English abstract). Published thesis.

Litvinovsky BA, Steele IM and Wickham SM (2000) Silicic magma formation in overthickened crust: Melting of charnockite and leucogranite at 15, 20 and 25 kbar. *Journal of Petrology* **41**, 717–37. doi: 10.1093/petrology/41.5.717

Liu DY, Nutman AP, Compston W, Wu JS and Shen QH (1992) Remnants of ≥3800 Ma crust in the Chinese part of the Sino- Korean craton. *Geology* **20**, 339. doi: 10.1130/0091-7613(1992)020<0339:ROMCIT>2.3.CO;2

Liu J, Li S, Zhu K and Zhao Q (2019) Geochronology, geochemistry and tectonic setting of the Guanmenshan Pluton in Benxi, Eastern Liaoning Province. *Earth Science* **45**, 869–979. doi: 10.3799/dqkx.2019.064

Liu J, Shen L, Ji M, Guan HM, Zhang ZC and Zhao ZD (2013) The Liaonan/Wanfu metamorphic core complexes in the Liaodong Peninsula: two stages of exhumation and constraints on the destruction of the North China Craton. *Tectonics* **32**, 1121–41. doi: 10.1002/tect.20064

Liu JL, Davis GA, Zhiyong L and Wu FY (2005) The Liaonan metamorphic core complex, Southeastern Liaoning Province, North China: a likely contributor to Cretaceous rotation of Eastern Liaoning, Korea and contiguous areas. *Tectonophysics* **407**, 65–80. doi: 10.1016/j.tecto.2005.07.001

Liu JL, Ji M, Shen L, Guang HM and Davis GA (2011) Early Cretaceous extensional structures in the Liaodong Peninsula: structural associations, geochronological constraints and regional tectonic implications. *Science China Earth Sciences* **54**, 823–42. doi: 10.1007/s11430-011-4189-y

Liu JX, Guo W and Zhu K (2016) Geochronology, geochemistry and geological significance of the Early Cretaceous intrusive rocks from Xiuyan area, eastern Liaoning Province. *Acta Petrologica Sinica* **32**, 2889–900 (in Chinese with English abstract).

Liu Y, Hu Z, Gao S, Günther D, Xu J, Gao CG and Chen HH (2008) In situ analysis of major and trace elements of anhydrous minerals by LA-ICP-MS without applying an internal standard. *Chemical Geology* **257**, 34–43. doi: 10.1016/j.chemgeo.2008.08.004

Liu Y, Wei J, Zhang D, Chen JJ and Zhang XM (2020) Early Cretaceous Wulong intermediate-mafic dike swarms in the Liaodong Peninsula: implications for rapid lithospheric delamination of the North China Craton. *Lithos* **362–363**, 1–23. doi: 10.1016/j.lithos.2020.105473

Lu XP (2004) Paleoproterozoic tectonic and magmatic events in Tonghu area. Ph.D. thesis. Jilin University, China (in Chinese with English abstract). Published thesis.

Ludwig KR (2003) *ISOPLOT 3.00: a geochronological toolkit for Microsoft Excel.* Berkeley: Berkeley Geochronology Center, Special Publication.

Martin H (1999) Adakitic magmas: modern analogues of Archaean granitoids. *Lithos* **46**, 411–29. doi: 10.1016/S0024-4937(98)00076-0

Menzies M, Xu Y, Zhang H and Fan W (2007) Integration of geology, geophysics and geochemistry: a key to understanding the North China Craton. *Lithos* **96**, 1–21. doi: 10.1016/j.lithos.2006.09.008

Menzies MA, Fan WM and Zhang M (1993) Palaeozoic and Cenozoic lithoprobe and the loss of N120 km of Archean lithosphere, Sino-Korean craton, China. In *Magmatic Processes and Plate Tectonics* (eds HM Prichard, T Alabaster, NBW Harris and CR Neary), pp. 71–81. Geological Society of London, Special Publication no. 76.

Moyen JF (2009) High Sr/Y and La/Yb ratios: the meaning of the "adakitic signature". *Lithos* **112**, 556–74. doi: 10.1016/j.lithos.2009.04.001

Muir RJ, Weaver SD, Bradshaw JD, Eby GN and Evans JA (1995) The Cretaceous separation point batholith, New Zealand: granitoid magmas formed by melting of mafic lithosphere. *Journal of the Geological Society of London* **152**, 689–701. doi: 10.1144/gsjgs.152.4.0689

Nash WP and Crecraft HR (1985) Partition coefficients for trace elements in silicic magmas. *Geochimica et Cosmochimica Acta* **49**, 2309–22. doi: 10.1016/0016-7037(85)90231-5

Niu YL, Liu Y, Xue QQ, Shao FL, Chen S, Duan M, Guo PY, Gong HM, Hu Y, Hu ZX, Kong JJ, Li JY, Liu JJ, Sun P, Sun WL, Ye L, Xiao YY and Zhang Y (2015) Exotic origin of the Chinese continental shelf: new insights into the tectonic evolution of the western Pacific and eastern China since the Mesozoic. *Science Bulletin* **60**, 1598–616. doi: CNKI:SUN:JXTW.0.2015-18-009

Othman DB, White WM and Patchett J (1989) The geochemistry of marine sediments, island arc magma genesis, and crust-mantle recycling. *Earth and Planetary Science Letters* **94**, 1–21. doi: 10.1016/0012-821X(89)90079-4

Patiño Douce AE and Beard JS (1995) Dehydration-melting of biotite gneiss and quartz amphibolite from 3 to 15 kbar. *Journal of Petrology* **36**, 707–38. doi: 10.1093/petrology/36.3.707

Pearce JA, Harris NBW and Tindle AG (1984) Trace element discrimination diagrams for the tectonic interpretation of granitic rocks. *Journal of Petrology* **4**, 956–83. doi: 10.1093/petrology/25.4.956

Peccerillo A and Taylor SR (1976) Geochemistry of Eocene calc-alkaline volcanic rocks from the Kastamonu area, Northern Turkey. *Contributions to Mineralogy and Petrology* **58**, 63–81. doi: 10.1007/BF00384745

Petford N and Atherton M (1996) Na-rich partial melts from newly underplated basaltic crust: the Cordillera Blanca Batholith, Peru. *Journal of Petrology* **37**, 1491–521. doi: 10.1093/petrology/37.6.1491

Plank T (2005) Constraints from thorium/lanthanum on sediment recycling at subduction zones and the evolution of the continents. *Journal of Petrology* **46**, 921–44. doi: 10.1093/petrology/egi005

Rudnick RL and Fountain DM (1995) Nature and composition of the continental crust: a lower crustal perspective. *Reviews of Geophysics* **33**, 267–309. doi: 10.1029/95RG01302

Rudnick RL, McLennan SM and Taylor SR (1985) Large ion lithophile elements in rocks from high-pressure granulite facies terrains. *Geochimica et Cosmochimica Acta* **49**, 1645–55. doi: 10.1016/0016-7037(85)90268-6

Sen C and Dunn T (1994) Dehydration melting of a basaltic composition amphibolite at 1.5 and 2.0 GPa: implications for the origin of adakites. *Contributions to Mineralogy Petrology* **117**, 394–409. doi: 10.1007/BF00307273

Skjerlie KP and Johnston AD (1993) Fluid-absent melting behavior of an F-rich tonalitic gneiss at mid-crustal pressures: implications for the generation of anorogenic granites. *Journal of Petrology* **34**, 785–815. doi: 10.1093/petrology/34.4.785

Stern CR and Kilian R (1996) Role of the subducted slab, mantle wedge and continental crust in the generation of adakites from the Andean Austral Volcanic Zone. *Contributions to Mineralogy Petrology* **123**, 263–81. doi: 10.1007/s004100050155

Sun DY, Suzuki K, Wu FY and Lu XP (2005) Chime dating and its application from Mesozoic granites of Huanggoushan, Jilin province. *Geochimica* **34**, 305–314. doi: CNKI:SUN:DQHX.0.2005-04-001

Sun JF and Yang JH (2009) Early Cret aceous A-type granites in the eastern North China Block with relation to destruct ion of the craton. *Journal of China University of Geoscience* **34**, 137–147 (in Chinese with English abstract).

Sun SS and McDonough WF (1989) Chemical and isotopic systematics of oceanic basalts: implications for mantle composition and processes. In *Magmatism in the Ocean Basins* (eds AD Saunders and MJ Norry), pp. 313–45. Geological Society of London, Special Publication no. **42**. doi: 10.1144/GSL.SP.1989.042.01.19

Sun W, Ding X, Hu YH and Li XH (2007) The golden transformation of the Cretaceous plate subduction in the west Pacific. *Earth Planetary Science Letters* **262**, 533–42. doi: 10.1016/j.epsl.2007.08.021

Wang K, Burov E, Gumiaux C, Chen Y, Lu G, Mezri L and Zhao L (2015) Formation of metamorphic core complexes in non-over-thickened continental crust: a case study of Liaodong Peninsula (East Asia). *Lithos* **238**, 86–100. doi: 10.1016/j.lithos.2015.09.023

Wang Q, McDermott F, Xu JF, Bellon H and Zhu YT (2005) Cenozoic K-rich adakitic volcanic rocks in the Hohxil area, northern Tibet: lower-crustal melting in an intracontinental setting. *Geology* **33**, 465–8. doi: 10.1130/G21522.1

Wang Q, Wyman DA, Xu J, Zhao Z, Li C, Wei X, Ma J and He B (2007) Early Cretaceous adakitic granites in the Northern Dabie Complex, central China: implications for partial melting and delamination of thickened lower crust. *Geochimica et Cosmochimica Acta* **71**, 2609–36. doi: 10.1016/j.gca.2007.03.008

Wang Q, Xu JF, Zhao ZH, Bao ZW, Xu W and Xiong XL (2004a) Cretaceous high-potassium intrusive rocks in the Yueshan-Hongzhen area of east China: adakites in an extensional tectonic regime within a continent. *Geochemical Journal* **38**, 417–34. doi: 10.2343/geochemj.38.417

Wang Q, Zhao ZH, Bao ZW, Xu JF, Liu W, Li CF, Bai ZH and Xiong XL (2004b) Geochemistry and petrogenesis of the Tongshankou and Yinzu adakitic intrusive rocks and the associated porphyry copper-molybdenum mineralization in southeast Hubei, east China. *Resource Geology* **54**, 137–52. doi: 10.1111/j.1751-3928.2004.tb00195.x

Wareham CD, Millar LL and Vaughan APM (1997) The generation of sodic granite magmas, western Palmer Land, Antarctic Peninsula. *Contributions to Mineralogy and Petrology* **128**, 81–96. doi: 10.1007/s004100050295

Wilson M (1989) *Igneous Petrogenesis.* London: Unwim Hyman, 366 p.

Windley BF, Maruyama S and Xiao WJ (2010) Delamination/thinning of subcontinental lithospheric mantle under eastern China: the role of water and multiple subduction. *American Journal of Science* **310**, 1250–93. doi: 10.2475/10.2010.03

Wu FY, Lin JQ, Wilde SA, Sun DY and Yang JH (2005a) Nature and significance of the early Cretaceous giant igneous event in eastern China. *Earth Planetary Science Letters* **233**, 103–19. doi: 10.1016/j.epsl.2005.02.019

Wu FY, Xu YG, Gao S and Zheng JP (2008) Lithospheric thinning and destruction of the North China Craton. *Acta Petrologica Sinica* **24**, 1145–74 (in Chinese with English abstract). doi: 10.1016/j.sedgeo.2008.03.008

Wu FY, Yang JH, Wilde SA and Zhang XO (2005b) Geochronology, petrogenesis and tectonic implications of Jurassic granites in the Liaodong Peninsula, NE China. *Chemical Geology* **221**, 127–56. doi: 10.1016/j.chemgeo.2005.04.010

Wu FY, Yang JH, Xu YG, Wilde SA and Walker RJ (2019) Destruction of the north China craton in the mesozoic. *Annual Review of Earth and Planetary Sciences* **47**, 173–95. doi: 10.1146/annurev-earth-053018-060342

Wu FY, Yang YH, Xie LW, Yang JH and Xu P (2006) Hf isotopic compositions of the standard zircons and baddeleyites used in U-Pb geochronology. *Chemical Geology* **234**, 105–26. doi: 10.1016/j.chemgeo.2006.05.003

Xiao QH, Li Y, Feng YF, Qiu RZ and Zhang Y (2010) A preliminary study of the relationship between Mesozoic lithosphere evolution in eastern China and the subduction of the Pacific plate. *Geology of China* **37**, 1092–101 (in Chinese with English abstract).

Xin W, Sun FY, Zhang YT, Fan X.Z and Li L (2019) Mafic–intermediate igneous rocks in the East Kunlun Orogenic Belt, northwestern China: Petrogenesis and implications for regional geodynamic evolution during the Triassic. *Lithos* **346–347**, 105–59. doi: 10.1016/j.lithos.2019.105159

Xiong XL, Adam J and Green TH (2005) Rutile stability and rutile/melt HFSE partitioning during partial melting of hydrous basalt: Implications for TTG genesis. *Chemical Geology* **210**, 339–59. doi: 10.1016/j.chemgeo.2005.01.014

Xiong XL, Liu XC and Zhu ZM (2011) Adakitic rocks and destruction of the North China Craton: evidence from experimental petrology and geochemistry. *Science China Earth Sciences* **54**, 858–70. doi: 10.1007/s11430-010-4167-9

Xu HJ, Ma CQ and Zhang JF (2012) Generation of Early Cretaceous High-Mg adakitic host and enclaves by magma mixing, Dabie orogen, Eastern China. *Lithos* **142–143**, 182–200. doi: 10.1016/j.lithos.2012.03.004

Xu W, Gao S, Wang Q, Wang DY and Liu YS (2006a) Mesozoic crustal thickening of the eastern North China craton: Evidence from eclogite xenoliths and petrologic implications. *Geology* **34**, 721–4. doi: 10.1130/G22551.1

Xu WL, Wang QH, Wang DY, Guo JH and Pei FP (2006b) Mesozoic adakitic rocks from the Xuzhou-Suzhou area, eastern China: Evidence for partial melting of delaminated lower continental crust. *Journal of Asian Earth Sciences* **27**, 230–40. doi: 10.1016/j.jseaes.2005.03.010

Xu YG, Li HY, Pang CJ and He B (2009) On the timing and duration of the destruction of the North China Craton. *Chinese Science Bulletin* **54**, 3379–96. doi: 10.1007/s11434-009-0346-5

Xu YG, Ma JL, Huang XL, Iizuka Y, Chung SL, Wang YB and Wu XY (2004) Early Cretaceous gabbroic complex from Yinan, Shandong Province: Petrogenesis and mantle domains beneath the North China Craton. *International Journal of Earth Sciences* **93**, 1025–41. doi: 10.1007/s00531-004-0430-7

Yang JH, Sun JF, Chen FK, Wilde SA and Wu FY (2007a) Sources and petrogenesis of Late Triassic dolerite dikes in the Liaodong Peninsula: implications for postcollisional lithosphere thinning of the eastern North China Craton. *Journal of Petrology* **48**, 1973–97. doi: 10.1093/petrology/egm046

Yang JH, Sun JF, Zhang JH and Wilde SA (2012) Petrogenesis of Late Triassic intrusive rocks in the northern Liaodong Peninsula related to decratonization of the North China Craton: Zircon U-Pb age and Hf-O isotope evidence. *Lithos* **153**, 108–28. doi: 10.1016/j.lithos.2012.06.023

Yang JH, Wu FY, Wilde SA and Liu XM (2007b) Petrogenesis of Late Triassic granitoids and their enclaves with implications for post-collisional lithospheric thinning of the Liaodong Peninsula, North China Craton. *Chemical Geology* **242**, 155–75. doi: 10.1016/j.chemgeo.2007.03.007

Yang JH, Wu FY, Zhang YB, Zhang Q and Wilde SA (2004) Zircons of Neoproterozoic age from Triassic diabase in southern Liaodong Peninsula. *China Science Bulletin* **49**, 1878–82. doi: 10.3321/j.issn:0023-074X.2004.18.011

Yang YH, Wu FY, Wilde SA, Liu XM, Zhang YB and Xie LW (2009) In situ perovskite Sr-Nd isotopic constraints on the petrogenesis of the Ordovician Mengyin kimberlites in the North China Craton. *Chemical Geology* **264**, 24–42. doi: 10.1016/j.chemgeo.2009.02.011

Yuan HL, Gao S, Dai MN, Zong CL, Günther D, Fontaine GH, Liu XM and Diwu CR (2008) Simultaneous determinations of U-Pb age, Hf isotopes and trace element compositions of zircon by excimer laser-ablation quadrupole and multiple-collector ICP-MS. *Chemical Geology* **247**, 100–18. doi: 10.1016/j.chemgeo.2007.10.003

Zhai M, Fan Q, Zhang H, Sui JL and Shao JA (2007) Lower crustal processes leading to Mesozoic lithospheric thinning beneath eastern North China: underplating, replacement and delamination. *Lithos* **96**, 36–54. doi: 10.1016/j.lithos.2006.09.016

Zhai MG and Santosh M (2011) The early Precambrian odyssey of the North China Craton: a synoptic overview. *Gondwana Research* **20**, 6–25. doi: 10.1016/j.gr.2011.02.005

Zhang J, Zhao ZF, Zheng YF and Dai MN (2010) Postcollisional magmatism: geochemicalconstraints on the petrogenesis of Mesozoic granitoids in the Sulu orogen, China. *Lithos* **119**, 512–36. doi: 10.1016/j.lithos.2010.08.005

Zhang Q (2013) Is the Mesozoic magmatism in eastern China related to the westward subduction of the Pacific plate. *Acta Petrologica et Mineralogica* **32**, 113–28 (in Chinese with English abstract).

Zhang Q and Wang Y (2001) The characteristics and tectonic metallogenic significances of the adakites in Yanshan period from eastern China. *Acta Petrologica Sinica* **17**, 236–44 (in Chinese with English abstract).

Zhao G, Sun M, Wilde SA and Sanzhong L (2005) Late Archean to Paleoproterozoic evolution of the North China Craton: key issues revisited. *Precambrian Research* **136**, 177–202. doi: 10.1016/j.precamres.2004.10.002

Zheng J, Griffin WL, O'Reilly SY, Yang JS, Li TF, Zhang M, Zhang RY and Liou JG (2006) Mineral chemistry of peridotites from Paleozoic, Mesozoic and Cenozoic lithosphere: constraints on mantle evolution beneath Eastern China. *Journal of Petrology* **47**, 2233–56. doi: 10.1093/petrology/egl042

Zheng JP, Griffin WL, O'Reilly SY, Yu CM, Zhang HF, Pearson N and Zhang M (2007) Mechanism and timing of lithospheric modification and replacement beneath the eastern North China Craton: peridotitic xenoliths from the 100 Ma Fuxin basalts and a regional synthesis. *Geochimica et Cosmochimica Acta* **71**, 5203–25. doi: 10.1016/j.gca.2007.07.028

Zheng YF, Chen RX, Xu Z and Zhang SB (2016) The transport of water in subduction zones. *Science China Earth Sciences* **59**, 651–82. doi: 10.1007/s11430-015-5258-4

Zheng YF, Xu Z, Zhao ZF and Dai LQ (2018) Mesozoic mafic magmatism in North China: implications for thinning and destruction of cratonic lithosphere. *Science China Earth Sciences* **61**, 353–85. doi: 10.1007/s11430-015-5258-4

Zhu RX, Chen L, Wu FY and Liu JL (2011) Timing, scale and mechanism of the destruction of the North China Craton. *Science China Earth Sciences* **54**, 789–97. doi: 10.1007/s11430-011-4203-4

Zhu RX and Xu YG (2019) The subduction of the west Pacific plate and the destruction of the North China Craton. *Science China Earth Sciences* **62**, 1340–50. doi: 10.1007/s11430-018-9356-y

Zhu RX, Yang JH and Wu FY (2012) Timing of destruction of the North China Craton. *Lithos* **149**, 51–60. doi: 10.1016/j.lithos.2012.05.013